Peremennye Zvezdy (*Variable Stars*) **42**, No. 9, 2022

Received 24 October; accepted 2 November.

DOI: 10.24412/2221-0474-2022-42-51-59

CCD Photometry of Young Stars AS 205 (V866 Sco), V1082 Cyg, and AS 310

Ulvi Valiyev[1], Sabahattin Alishov[2], Nariman Ismailov [2]

[1] Batabat Astrophysical Observatory of Nakhichevan Branch of Azerbaijan National Academy of Sciences, Azerbaijan

[2] N. Tusi Shamakhy Astrophysical Observatory of Azerbaijan National Academy of Sciences, Shamakhy region, Azerbaijan

We present the results of BVR_cI_c CCD photometric observations of the classical T Tauri stars AS 205 (V866 Sco), V1082 Cyg and the HAeBe star AS 310 obtained in 2016–2022. Photometric variations of the star AS 310 with a large amplitude were reliably established for the first time, they are possibly due to binarity or multiplicity of the star. The scale of the star's activity differs from a year to year. Parameters of the upgraded photometric system, currently at use at the Shamahy Observatory, are described.

1 Introduction

In most cases, the brightness of classical T Tauri stars (CTTS) varies in a complex manner (Parenago, 1954; Herbst et al., 1994; Ismailov, 2005; Grankin, 2016). It is possible that irregular disk accretion in stars of this type causes an inhomogeneity of the stellar surface, so that the star's axial rotation can provide quasi-cyclic light variations. However, in some cases, the amplitude of light variation exceeds 1 mag, and the time scale of observed variations can be quite large. Therefore, it is desirable to obtain as many photometric observations of such objects as possible in order to conduct research in each specific case. In this work, the results of photometric observations of two CTTS and one Herbig AeBe (HAeBe) star, acquired in 2016–2022, are presented.

The CTTS AS 205 A = AS 205 N (V866 Sco) is a star of the spectral type K5 in a moderately bright ($V = 12\overset{\mathrm{m}}{.}4$) triple system. At an angular distance of $1\overset{''}{.}3$ from AS 205 N (corresponding to ≈180 a.u. at the distance of 140 pc), there is a low-mass K7–M0 spectroscopic binary AS 205 S (Ghez et al., 1993; Prato et al., 2003). Two stable periods ($P_1 = 6\overset{\mathrm{d}}{.}78$ and $P_2 = 24\overset{\mathrm{d}}{.}78$) are observed in the AS 205N light curve (Artemenko et al., 2010). The P_1 period is a typical one for CTTS and can be explained with the presence of cool spots on the stellar surface. The phase diagram of the P_2 period shows a modulation of brightness and color, indicating the presence of an additional cool source in the system. Since AS 205 N is about 2 times brighter than AS 205 S in the V band (Herbig & Bell, 1988), the observed brightness modulation ($\Delta V = 0\overset{\mathrm{m}}{.}25$) should be attributed to the main star. From the temperature and bolometric luminosity relations (Andrews et al., 2009), the mass of AS 205 N is expected to be about $0.9M_\odot$.

Table 1: **Results of photometric observations of AS 205 (V866 Sco)**

JD2450000+	B	JD2450000 +	V	JD2450000 +	R_c	JD2450000+	I_c
8667.2868	12.205	8667.2781	11.125	8667.2710	10.675	8667.2980	9.217
8668.2470	12.747	8668.2382	11.546	8668.2304	10.889	8668.2550	9.411
8669.2433	13.276	8669.2302	11.951	8669.2228	11.303	8669.2570	9.663
8687.2432	12.136	8687.2328	10.983	8670.3806	10.979	8687.2570	8.931
8688.2468	12.144	8688.2241	11.007	8672.3343	10.803	8688.2580	8.839
8695.2929	12.070	8695.2796	10.846	8687.2278	10.415	8695.3050	8.795
8998.3921	12.035	8700.2743	10.186	8688.2194	10.497	8700.2940	8.389
9000.3298	11.935	8712.1937	10.747	8695.2671	10.309	8712.2160	8.906
9013.3259	12.533	8998.3840	11.032	8700.2690	9.768	8998.4029	9.102
9017.2465	12.533	9000.3211	10.935	8712.1903	10.274	9000.3377	9.001
9024.2550	12.632	9013.3187	11.320	8998.3762	10.537	9024.2702	9.405
9047.3554	12.035	9014.2323	11.224	9000.3156	10.438	9047.3680	9.001
9049.2406	13.429	9017.2366	11.416	9012.3474	10.537	9049.2488	9.809
9349.3546	13.828	9019.2872	11.032	9013.3143	10.833	9349.3638	10.415
9351.3605	14.326	9024.2410	11.512	9014.2251	10.833	9351.3664	10.617
9352.3855	13.728	9047.3479	10.935	9017.2308	10.833	9352.3932	10.314
9367.2569	12.832	9049.2335	12.088	9019.2827	10.635	9367.2725	9.405
9368.2532	12.931	9349.3453	12.665	9024.2314	10.932	9368.2692	9.405
9382.3541	12.632	9351.3549	12.953	9047.3456	10.537	9382.3638	9.405
9385.3775	12.533	9352.3723	12.377	9049.2284	11.426	9385.3831	9.304
9386.3855	12.433	9367.2350	11.608	9349.3398	12.020	9386.3939	9.304
9399.2784	12.433	9368.2367	11.800	9351.3511	12.217	9399.2879	9.203
9400.2731	11.836	9382.3407	11.512	9352.3511	11.723	9400.2824	8.799
9401.2339	12.035	9385.3704	11.416	9367.2203	11.130	9401.2391	8.799
9407.2315	11.836	9386.3823	11.320	9368.2281	10.932	9407.2362	8.698
9411.3186	11.935	9399.2705	11.320	9382.3342	10.932	9411.3240	8.900
9413.2780	12.433	9400.2653	10.839	9385.3672	10.833	9412.3567	9.304
		9401.2280	10.839	9386.3797	10.734	9413.2864	9.102
		9407.2270	10.743	9399.2659	10.734		
		9411.3095	10.935	9400.2600	10.339		
		9412.3450	11.416	9401.2235	10.339		
		9413.2666	11.224	9407.2239	10.240		
				9411.3066	10.339		
				9412.3419	10.833		
				9413.2600	10.635		

Table 2: **Results of photometric observations of V 1082 Cyg**

JD2450000+	V	JD2450000+	B
8669.4194	13.004	8669.4249	14.197
8672.3626	12.715	8672.3681	13.799
8686.4394	13.296	8686.4448	14.547
8687.3276	12.980	8687.3333	14.140
8695.3362	13.173	8695.3509	14.500
8700.3563	13.122	8700.3699	14.369
9407.3367	12.822	9407.3424	13.933
9411.3383	13.251	9412.3779	14.552
9412.3744	13.305	9413.3411	14.385
9413.3345	13.199	9415.3452	14.315
9415.3384	13.138	9411.3441	14.524
9428.3491	13.003	9428.3574	14.188
9432.3191	12.993	9432.3275	14.134
9433.3068	13.067	9433.3149	14.237
9434.3348	13.027	9434.3431	14.179
9436.3553	12.780	9436.3641	13.858
9438.3355	13.136	9438.3417	14.322

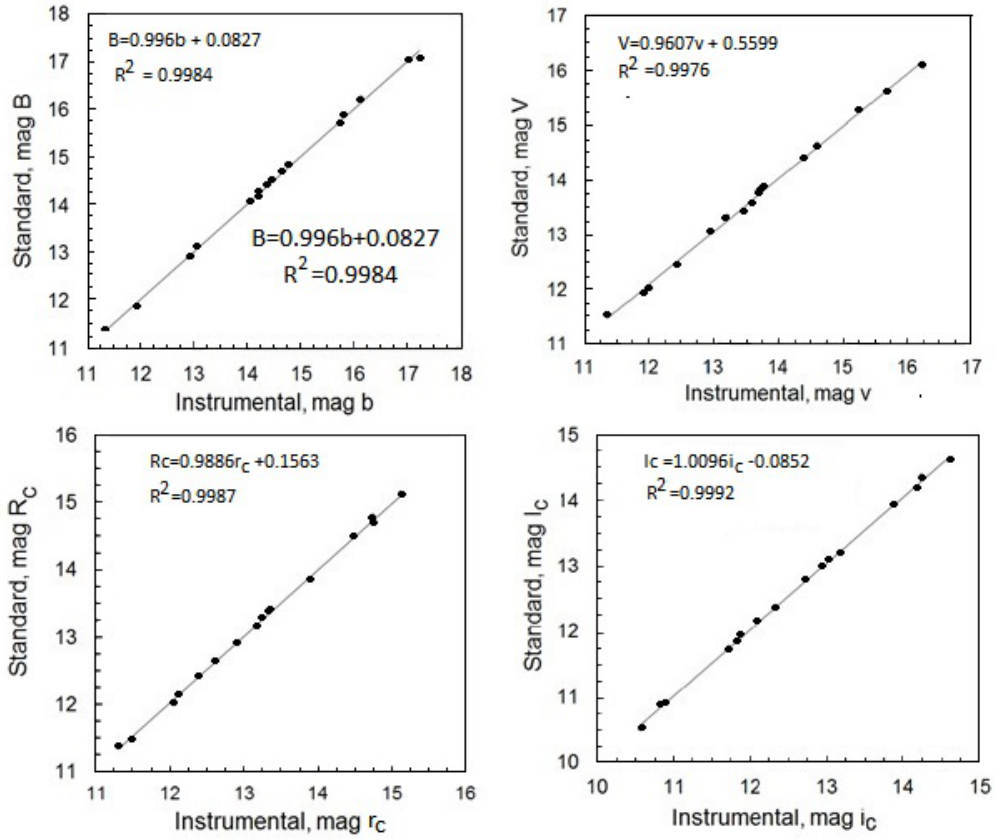

Figure 1.
Comparison of the international BVR_cI_c and ShAO instrumental photometric systems. The points are approximated by straight lines, the reliability coefficient is $R^2 = 0.998 \pm 0.001$.

V1082 Cyg (HBC 728) is considered a typical CTTS, with a distance to the star of 660 pc. The V brightness of the star is $13\overset{\text{m}}{.}3$. Due to its being relatively faint, this star remained poorly studied. In the catalog by Herbig & Bell (1988), its number is HBC 728. Grankin et al. (2007) found for the star an average variability amplitude of $0\overset{\text{m}}{.}828$. Percy et al. (2010), mentioning the stars's photographic magnitude range $13\overset{\text{m}}{.}8$ – $15\overset{\text{m}}{.}0$, determined the range of its periodic variations $\Delta V < 0\overset{\text{m}}{.}3$, the period being 22^{d}. There is no accurate measurement of the star's spectral type because of its strong emission lines. Its average effective temperature is estimated as 5500 K.

The V-band brightness of the Herbig AeBe star AS 310 (HBC 284) is $12\overset{\text{m}}{.}52$, and its variability is relatively poorly studied. No periodical brightness variations were detected (Percy et al., 2010). The spectral type of the star was determined as BIVe, with effective temperature at 25800 K (Hernández et al., 2004).

2 Observations

CCD photometry of the program stars was performed at the Cassegrain focus of the 60 cm Carl Zeiss telescope of the Shamakhy Astrophysical Observatory. As a light detector, an FLI 4 × 4 k CCD camera was used. The photometer is equipped with standard

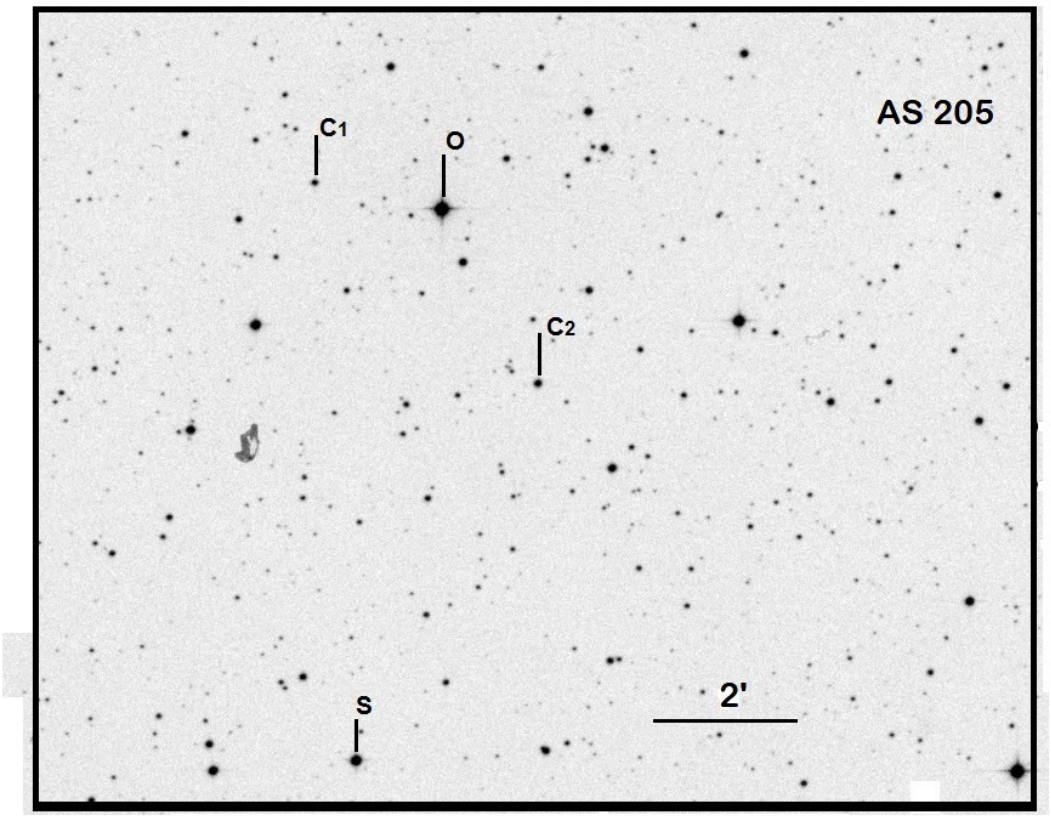

Figure 2.
The finding chart for the program star AS 205. O is the program object, S is the reference (standard) star, C1 and C2 are check stars.

BVR_cI_c filters. After the previous modification of the photometer (Abdullayev et al., 2012, and references therein), several of parameters of the system were improved. Since our observations were obtained using the upgraded system, this paper describes the new photometer+telescope system which is currently in use.

The telescope, with an aperture of 600 mm and equivalent focal length $F = 7500$ mm, has the scale in its focal plane $\mu = 27.5''$ per mm. Considering that the pixel size is 9μm and the number of pixels per side is 4096, the size of the useful part of the focal plane is approximately $17' \times 17'$.

With the given pixel size, we get $0''.247$ for single-pixel resolution. Depending on the seeing, 2×2 or 4×4 binning was used, corresponding respectively to $0''.49$ per pixel and $0''.99$ per pixel. The total area covered by the camera is approximately $30'$, and the effective linear area in the focal plane is $17' \times 17'$. Dark, bias, flat-field calibration images were regularly taken during observations.

To transfer the instrumental system to the international Johnson–Cousins system, transition coefficients were determined based on observations of Landolt standards (Landolt, 1992). Currently, standard star fields are listed in the European Southern Observatory (ESO) (https://www.eso.org/sci/observing/tools/standards/Landolt.html) directory. The fields with Landolt standards were selected so that the brightness of the standards located there was close to the brightness of the program stars.

Diagrams in Fig. 1 show comparison between the brightness of standard stars and

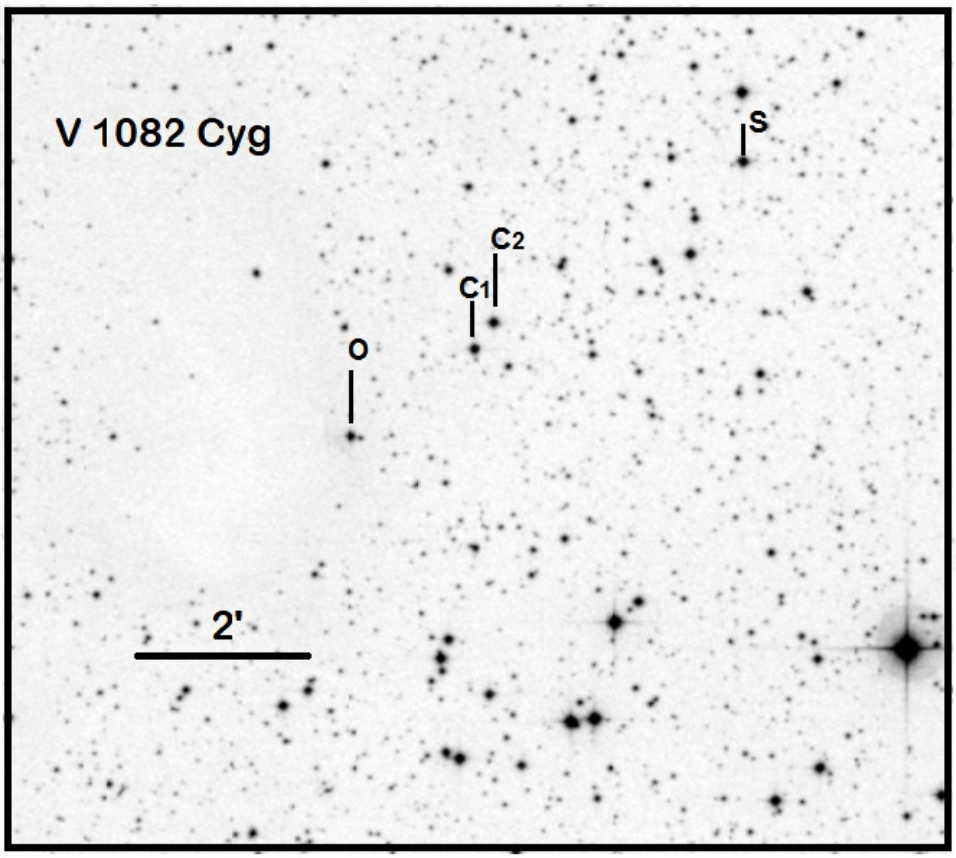

Figure 3.
The finding chart for the program star V1082 Cyg. Same designations as in Fig. 2.

the instrumental brightness measurements obtained in different bands. For each panel of Fig. 1, the corresponding transition formulas and the reliability coefficient R^2 of the approximating straight line are given. As can be seen, the transition coefficients allow us to reduce the results to the international system with a high accuracy.

The formulas for converting our instrumental system to the international BVR_cI_c system are the following:

$$B = 0.996b + 0.0827,$$

$$V = 0.9607v + 0.5599,$$

$$R_c = 0.9886r_c + 0.1563, \quad (1)$$

$$I_c = 1.0096i_c - 0.0852.$$

Here, the lowercase letters (right side) correspond to magnitudes in the instrumental system. When approximating the data, the reliability coefficient of passing a straight line through the data points was, on average, $R^2 = 0.998 \pm 0.001$.

All reductions of the observations were performed using the MaxIm DL software. Typical average measurement errors for individual bands are $\pm 0\overset{m}{.}008$ V, ± 0.01 R_c, $\pm 0\overset{m}{.}02$ I_c, and $\pm 0\overset{m}{.}03$ B.

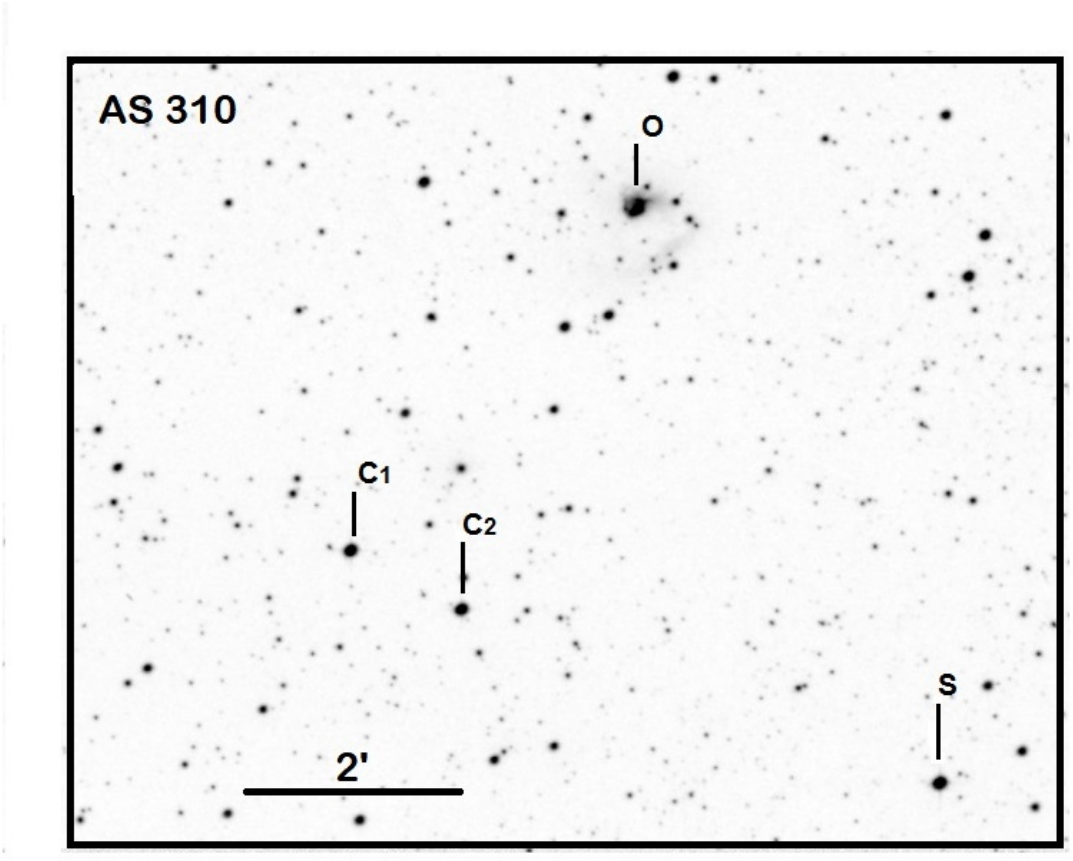

Figure 4.
The finding chart for the program star AS 310. Same designations as in Fig. 2.

Obtained observations

Our photometric measurements performed using the differential method. In Figs. 2–4, finding charts of the program stars are presented. R.m.s. errors of program-star photometry were determined with respect to standard and check stars. The magnitudes of the star AS 205 were determined relative to the reference star UCAC4 357-076076 whose magnitudes in each of the filters are the following: $B = 13\overset{m}{.}775$, $V = 12\overset{m}{.}912$, $R = 12\overset{m}{.}995$, $I = 11\overset{m}{.}808$. In order to check the stability of this star and the check stars C1 and C2, their magnitudes were derived relative to each other in different combinations in the available frames, and the stars showing stability in the derived errors were selected. The selected reference star (S) UCAC4 357-076076 and the check stars C1 and C2 are shown in Fig. 2. We used the same procedure for observations of the other program stars (Figs. 3–4). The mean rms of a measurement was calculated from photometric measurements of the check stars. In different filters, the following errors were found: $\pm 0\overset{m}{.}02$ B, $\pm 0\overset{m}{.}008$ V, $\pm 0\overset{m}{.}005$ R_c, $\pm 0\overset{m}{.}009$ I_c.

The results of our photometrical observations of the program stars are collected in Tables 1–3.

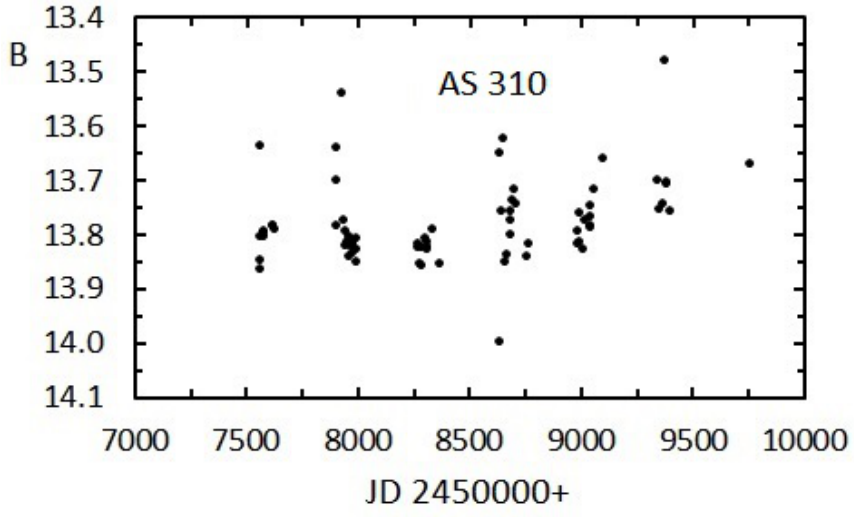

Figure 5.
The light curve of the star AS 310 in the B band for 2016–2022.

3 Conclusion

Of interest is the character of variations of the HBe star AS 310, observed in 2016–2022. Figure 5 presents its light curves in the B and V bands obtained in our observations. The maximal amplitudes registered in this time interval are $\Delta B \sim 0\overset{m}{.}4$, $\Delta V \sim 0\overset{m}{.}6$. Remarkably, the largest amplitude was observed for AS 310 in 2018 in the V band. Unfortunately, at that time we did not observed the star in the B band as frequently as in the V band. Our observations show that, unlike other HAeBe stars, AS 310 has an unusually large amplitude of brightness variations, possibly due to the binarity or multiplicity of the star. The star's activity was different in different years of our observations. To clarify these findings, additional long-term observations of the star are needed.

References:

Abdullayev, B. I., Alekberov, I. A., Gulmaliyev, N. I., et al., 2012, *Azerbaijan Astron. J.*, No. 4, 39
Andrews, S. M., Wilner, D. J., Hughes, A. M., et al., 2009, *Astrophys. J.*, **700**, 1502
Artemenko, S. A., Grankin, K. N., Petrov, P. P., 2010, *Astron. Reports*, **54**, 163
Ghez, A. M., Neugebauer, G., Matthews, K., 1993, *Astron. J.*, **106**, 2005
Grankin, K. N., Melnikov, S. Yu., Bouvier, J., et al., 2007, *Astron. & Astrophys.*, **461**, 183
Grankin, K. N., 2016, *Astron. Letters*, **42**, 314
Herbig, G. H., Bell, K. R., 1988, *Lick Obs. Bull.*, No. 1111, 90
Herbst, W., Herbst, D., Grossman, E. J., Weinstein D., 1994, *Astrophys. J.*, **108**, 1906
Hernández, J., Calvet, N., Briceño, C., et al., 2004, *Astron. J.*,**127**, 1682
Ismailov, N. Z., 2005, *Astron. Reports*, **49**, 309
Landolt, A. U., 1992, *Astron. J.*, **104**, 340
Parenago, P., 1954, *Publ.Sternberg Astron. Inst.*,**25**, 222
Percy, J. R., Grynko, S., Seneviratne, R., 2010, *Publ. Astron. Soc. Pacific*, **122**, 753
Prato, L., Greene, T. P., Simon, M., 2003, *Astrophys. J.*, **584**, 853

Table 3: **Results of photometric observations of AS 310**

JD2450000+	V	JD2450000+	B
7569.3330	12.597	7569.3399	13.867
7569.3330	12.576	7569.3698	13.849
7569.4000	12.516	7570.3306	13.639
7570.3215	12.541	7570.3714	13.805
7570.3558	12.57	7584.2553	13.805
7584.2468	12.578	7585.2246	13.795
7585.2167	12.561	7586.3354	13.797
7586.3269	12.556	7620.1753	13.784
7620.1634	12.566	7624.1615	13.786
7620.1634	12.566	7628.1647	13.792
7624.1495	12.568	7910.2968	13.784
7626.3037	12.579	7911.2919	13.7
7628.1533	12.572	7911.3212	13.642
7910.2903	12.456	7936.2791	13.54
7911.2831	12.504	7938.3675	13.776
7911.3120	12.506	7951.3596	13.795
7936.2703	12.497	7952.2956	13.823
7938.3634	12.438	7955.1953	13.816
7951.3555	12.568	7961.2232	13.806
7952.2916	12.493	7962.2825	13.843
7955.1910	12.467	7963.2602	13.817
7961.2063	12.51	7965.2437	13.812
7962.2658	12.476	7972.2497	13.822
7963.2434	12.544	7973.2508	13.815
7996.1412	12.436	7974.2888	13.823
7973.2421	12.372	7978.1974	13.82
7974.2824	12.401	7979.1885	13.834
7977.2798	12.331	7994.2075	13.81
7978.1768	12.46	7995.1730	13.851
7979.1821	12.464	7996.1473	13.829
7994.1621	12.473	8275.3799	13.825
7995.1650	12.561	8276.3979	13.819
7996.1412	12.436	8291.3184	13.825
8275.3731	11.96	8292.2783	13.858
8276.3915	12.463	8302.3258	13.807
8285.4671	12.524	8285.4698	13.856
8291.3087	12.217	8310.3949	13.83
8292.2686	12.458	8311.3631	13.814
8302.3162	12.185	8315.3129	13.824
8306.4274	12.555	8315.3129	13.824
8309.3293	12.456	8338.2313	13.793
8310.3832	12.41	8369.2742	13.855
8311.3528	12.248	8636.3581	14
8312.3731	12.559	8637.3359	13.652
8315.3033	12.557	8649.3425	13.76
8338.2139	12.442	8655.3121	13.625
8348.3669	12.489	8660.2863	13.852
8365.1863	12.542	8669.2950	13.839
8369.2558	12.146	8687.3021	13.776
8637.3296	12.364	8688.2861	13.757
8649.3370	12.39	8689.3819	13.802
8655.2988	12.272	8695.2378	13.737
8660.2736	12.436	8700.2280	13.718
8669.2800	12.527	8712.2634	13.744
8687.2914	12.543	8759.1823	13.843
8688.2751	12.529	8771.1540	13.818
8689.3710	12.468	8991.3612	13.794
8695.2202	12.365	8992.3337	13.819
8700.2120	12.464	8998.3562	13.763
8712.2513	12.400	9000.3697	13.814
8719.3680	12.507	9012.3312	13.83
8759.1694	12.337	9017.3509	13.774

Table 3: **Continued**

JD2450000+	V	JD2450000+	B
8771.1417	12.333	9046.3425	13.768
8991.3495	12.373	9047.3972	13.79
8992.3214	12.553	9048.4247	13.784
8998.3471	12.543	9049.3249	13.748
9000.3579	12.591	9058.3614	13.718
9012.3224	12.501	9101.2057	13.66
9017.3389	12.564	9349.3999	13.7
9046.3329	12.551	9351.3924	13.756
9047.3878	12.515	9368.3058	13.745
9048.4088	12.414	9382.3961	13.479
9049.3188	12.539	9384.4028	13.705
9058.3535	12.504	9385.4003	13.707
9101.2005	12.502	9399.2464	13.760
9351.3861	12.532	9762.2863	13.671
9368.2946	12.476		
9382.3857	12.458		
9384.3968	12.511		
9385.3948	12.524		
9399.2381	12.534		
9762.2738	12.437		